GeoHealth

RESEARCH ARTICLE
10.1029/2020GH000351

Special Section:
The COVID-19 pandemic: linking health, society and environment

Key Points:
- The COVID-19 lockdown provides an opportunity to assess the impact of air pollution from the Indo-Gangetic Plain on the Himalaya.
- Air pollutions levels in cities in the western Indo-Gangetic Plain experienced marked drops that coincided with the lockdown.
- Across the Indo-Gangetic Plain and Himalaya, there were reductions in air pollution in the west and increases in the east.

Correspondence to:
G. W. K. Moore,
gwk.moore@utoronto.ca

Citation:
Moore, G. W. K., & Semple, J. L. (2021). Himalaya air quality impacts from the COVID-19 lockdown across the Indo-Gangetic Plain. *GeoHealth*, *5*, e2020GH000351. https://doi.org/10.1029/2020GH000351

Received 10 NOV 2020
Accepted 10 MAR 2021

Author Contributions:
Conceptualization: G. W. K. Moore, J. L. Semple
Data curation: G. W. K. Moore
Formal analysis: G. W. K. Moore
Methodology: G. W. K. Moore, J. L. Semple
Validation: G. W. K. Moore
Visualization: G. W. K. Moore
Writing – original draft: G. W. K. Moore
Writing – review & editing: G. W. K. Moore, J. L. Semple

Himalaya Air Quality Impacts From the COVID-19 Lockdown Across the Indo-Gangetic Plain

G. W. K. Moore[1,2] and J. L. Semple[3]

[1]Department of Physics, University of Toronto, Toronto, ON, Canada, [2]Department of Chemical and Physical Sciences, University of Toronto Mississauga, Mississauga, ON, Canada, [3]Department of Surgery, University of Toronto, Toronto, ON, Canada

Abstract Starting in January 2020, the novel coronavirus, now known as acute respiratory syndrome coronavirus (SARS-CoV-2) and the disease that it causes (COVID-19) has had significant impacts on human health, the environment, and the economy globally. The rapid lockdown that occurred as well as its well documented timing allows for an unprecedented opportunity to examine the impact of air pollution from densely populated regions has on adjacent and pristine environments. Here, we use in situ and satellite observations to show that there was a step function decrease in two key indicators of air quality, nitrogen dioxide and airborne particulates, in locations within the Indo-Gangetic Plan (IGP) as a result of the Spring 2020 lockdown. Based on anomaly patterns, we find a dipole response with a statistically significant reduction in air pollution along the western IGP and Himalaya and an increase in air pollution in the eastern IGP and Himalaya. We show that spatial variability in the reductions in economic activity across northern India and the adjoining countries of Nepal, Pakistan, and Bangladesh contributed to this dipole as did a persistent atmospheric circulation anomaly across the region during the lockdown.

1. Introduction

The densely populated IGP that includes much of northern India, eastern Pakistan and Bangladesh, is one of the most polluted regions of the world (Lau & Kim, 2010). Please refer to Figure 1 for place names in the region of interest. For example, based on fine particle pollution data from 29 U.S. diplomatic posts across the world, New Delhi ranks as the most polluted city having median air quality rated as being unhealthy with the frequent occurrence of hazardous conditions (Dhammapala, 2019). Common sources of air pollution in the region include transportation, construction, industrial activity, electricity generation, waste burning, and biomass burning (Dhammapala, 2019; Ghude et al., 2011). There is evidence that this pollution has the potential for increasingly dramatic impacts, as the IGP continues to industrialize, on the population, environment and climate in the relatively pristine Himalaya that form the northern boundary of the IGP (Bonasoni et al., 2012; Dentener et al., 2006; Ghude et al., 2011; Moore & Semple, 2009). An example of such an event, that occurred on December 5, 2017, where pollution from the IGP was observed to encroach on the Himalaya is shown in Figure 2.

One common characteristic that spans most research topics in the geosciences is the inability to undertake large-scale controlled experiments that help identify processes and pathways. The existence of events characterized by step changes in external forcing often allow unique opportunities that mimic the sort of experiments that are common in laboratory-based scientific disciplines. Examples include: volcanic eruptions that result in large inputs of aerosols into the stratosphere that subsequently impact the earth's radiative balance leading to a widespread cooling (Brasseur & Granier, 1992); total solar eclipses that result in a transient reduction in incoming solar radiation that can impact meteorological processes throughout the atmospheric column (Aplin et al., 2016). There is also evidence that the cessation of air travel across the United States after September 11, 2001 resulted in a reduction in contrails that impacted surface temperatures (Travis et al., 2004). However, the relatively short period, 4 days, of the cessation limited the ability to definitively attribute the presence of a signal (Hong et al., 2008).

In a similar vein, the COVID-19 related lockdown (Chamas, 2020; Ellis-Petersen et al., 2020) that occurred across the IGP in March 2020 offers an unique opportunity to assess the impact of pollution sources across this region on the Himalaya. We will focus attention on Nitrogen Dioxide (NO_2), an important component

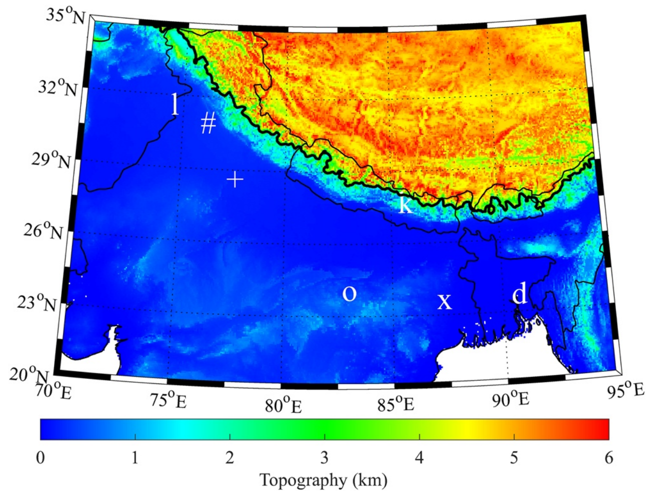

Figure 1. Topography (m) and place names in the region of intereast. The locations of New Delhi ("+"), Ludhiana ("#"), Singrauli ("o"), Asansol ("x"), Lahore ('l), Kathmandu ("k") and Dhaka ("d") are indicated. Political boundaries are shown by the thin black curves with the 3000 m topographic height shown by the thick black curve.

of air pollution (WHO, 2006) in and of itself as well as being a precursor species to ozone, a pollutant and oxidant that has been shown to impact lung function (Lippmann, 1989). We will also consider airborne particulate matter with diameters smaller than 2.5 μm (pm2.5) that have also been shown to impact human health (WHO, 2006).

Based on anomaly patterns, we find a dipole response during the Spring 2020 lockdown with a statistically significant reduction in air pollution along the western IGP and Himalaya as well as an increase in air pollution in the eastern IGP and Himalaya. We argue that spatial variability in the reductions in economic activity across northern India and the adjoining countries of Nepal, Pakistan, and Bangladesh contributed to this dipole as did a persistent atmospheric circulation anomaly across the region during the lockdown.

2. Data and Methods

Data on daily mean surface concentrations of NO_2 during the period of interest, December 1, 2019–May 1 2020, were accessed from OpenAQ Platform for the four locations discussed in the paper: Delhi, Ludhiana, Singrauli, and Asansol. Delhi had ~45 reporting sites that were averaged to obtain the time series for this location. All other locations had individual reporting sites. For the period of interest, data availability is greater than 98%. To develop a climatology for the surface concentration of NO_2 at Delhi, data from the OpenAQ Platform was accessed for the period 2017–2019 as well as data from the archives of the Central Pollution Control Board was accessed for the period 2005–2016. The multiple reporting sites were averaged to obtain the climatology for Delhi. The climatology did not include 2020 so as to not introduce a bias due to the observed low values during the lockdown.

Data on daily mean surface pm2.5 concentrations were obtained from United States Embassies or Consulates in Delhi India, Lahore Pakistan, Dhaka Bangladesh and Kathmandu Nepal as archived by the U.S. Environmental Protection Agency. For the period of interest, data availability was 100%. Data at Delhi is available back to 2016 and the data for the period 2016–2019 was used to develop a climatology for this location.

To characterize the impact of the lockdown on the spatial and temporal variability in air quality across the IGP and the Himalaya, we use daily tropospheric NO_2 column retrievals from the ozone monitoring instrument (OMI) instrument (Boersma et al., 2011) on National Aeronautics and Space Administration (NASA)'s Aura satellite as well as higher spatial resolution data from the TROPOspheric Monitoring (TROPOMI) instrument (Veefkind et al., 2012) on European Space Agency (ESA)'s Sentinel 5P satellite.

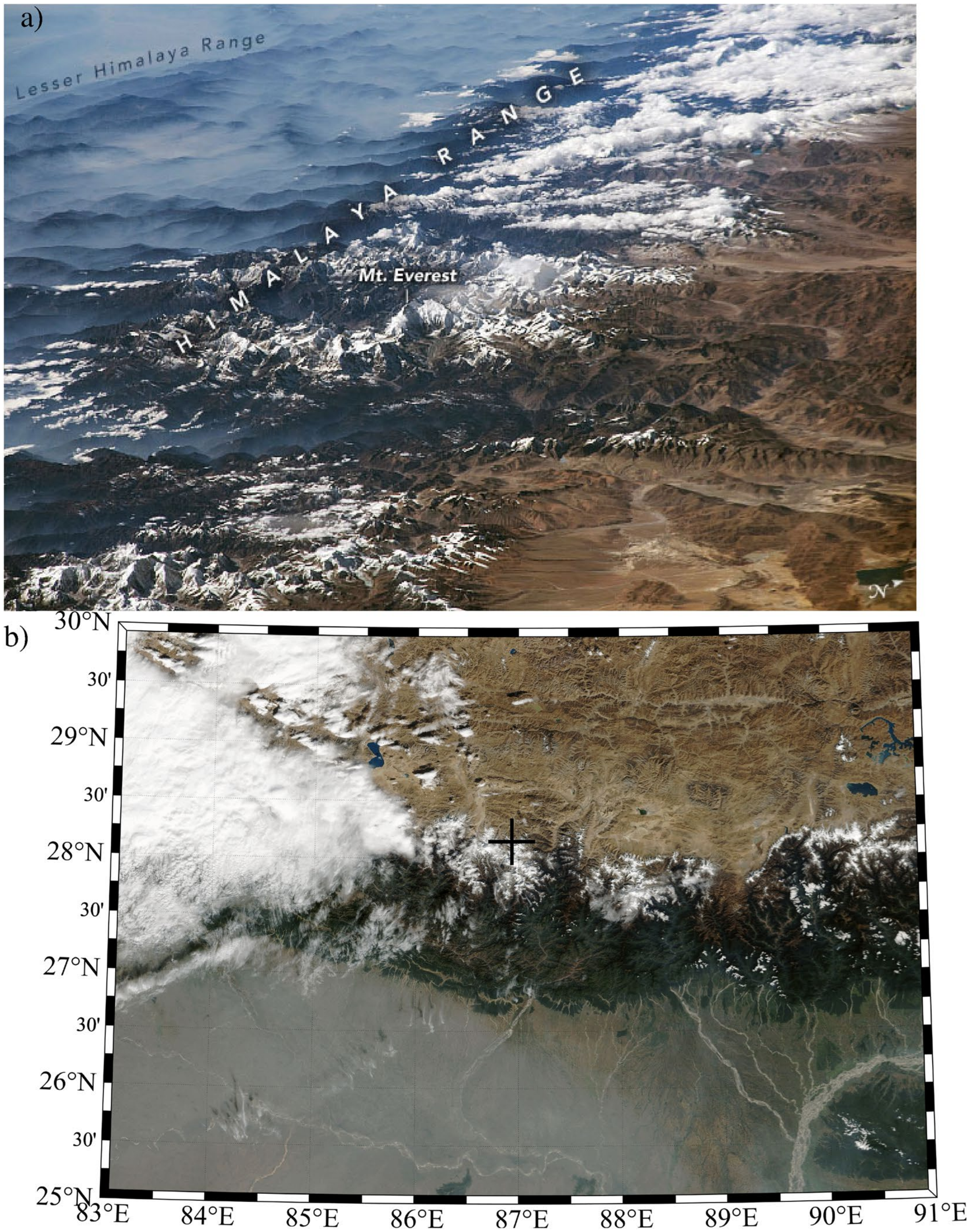

Figure 2. An example of pollution from the IGP's impact on the Himalaya. (a) Photograph of the Mount Everest region of the Himalaya taken on December 5, 2017 from the International Space Station. (b) MODIS true-color satellite image on the same day with Mount Everest indicated by the "+". In both images, pollution from the IGP can be seen to encroach on the Himalaya. IGP, Indo-Gangetic Plan; MODIS, Moderate Resolution Imaging Spectroradiometer. Images courtesy of NASA.

Daily tropospheric NO_2 column retrievals from the OMI instrument on NASA's Aura satellite, available from 2005 to 2020 at a spatial resolution of ¼° or ~25 km (Boersma et al., 2011), as well as the TROPOMI instrument on ESA's Sentinel 5P satellite, available from 2018 to 2020 at a spatial resolution of ~4 km (Veefkind et al., 2012) were used to characterize the spatial distribution of pollutants. For each data set, the cloud cleared retrievals were used. The 16 years length of data availability for the OMI instrument allows for the development of a climatology.

10.1029/2020GH000351

Information on the spatial distribution of particulate matter is also available from the OMI instrument through the so-called Aerosol Index (AI) that uses differential absorption of upwelling ultra-violet radiation to indicate the presence of aerosols associated with dust, smoke and volcanic ash (Torres et al., 2007). It is available at a spatial resolution of 1° daily from 2005 to 2020 (Torres et al., 2007).

Mass-weighted wind data from the European Centre for Medium-Range Weather Forecasts' ERA5 Reanalysis (Hersbach et al., 2020) were used to characterize the atmospheric circulation during April 2020. The data is available at a spatial resolution of ~30 km for the period 1979–2020.

3. Results

Figure 3 shows time series of the daily mean surface concentration of NO_2 at selected sites across the IGP. Please refer to Figure 1 for the locations of these sites. The data in this figure shows a step function reduction in surface NO_2 concentration occurred in both Delhi (Figure 3a) and Ludhiana (Figure 3b), large urban centers in the Indian sector of the IGP, around the middle of March that coincided with the lockdown in the region (Chamas, 2020; Ellis-Petersen et al., 2020). The reduction in surface NO_2 concentrations persisted through the end of April in these cities. For example, mean NO_2 values at Delhi and Ludhiana were 44 and 36 μg/m^3 for the period February 15–March 15, 2020 and at both locations, the mean over the period April 1–30, 2020 was 18 μg/m^3.

Climatological surface NO_2 data is available for Delhi back to 2005 and shows a seasonal decline in values during the transition from winter through the spring (Mohan & Kandya, 2007) that can also be seen in Figure 3a. A 31 days moving window smoother was applied to the climatological time series to reduce high frequency signals that are the result of their short length so as to allow a clearer picture of the seasonal cycle and its variability. This inter-annual variability in surface NO_2 concentration confirm that values recorded in Delhi during the lockdown were two standard deviations below the mean indicating highly anomalous conditions. Indeed, the monthly mean surface NO_2 concentration observed in Delhi during April 2020 was the lowest observed for the period 2005–2020.

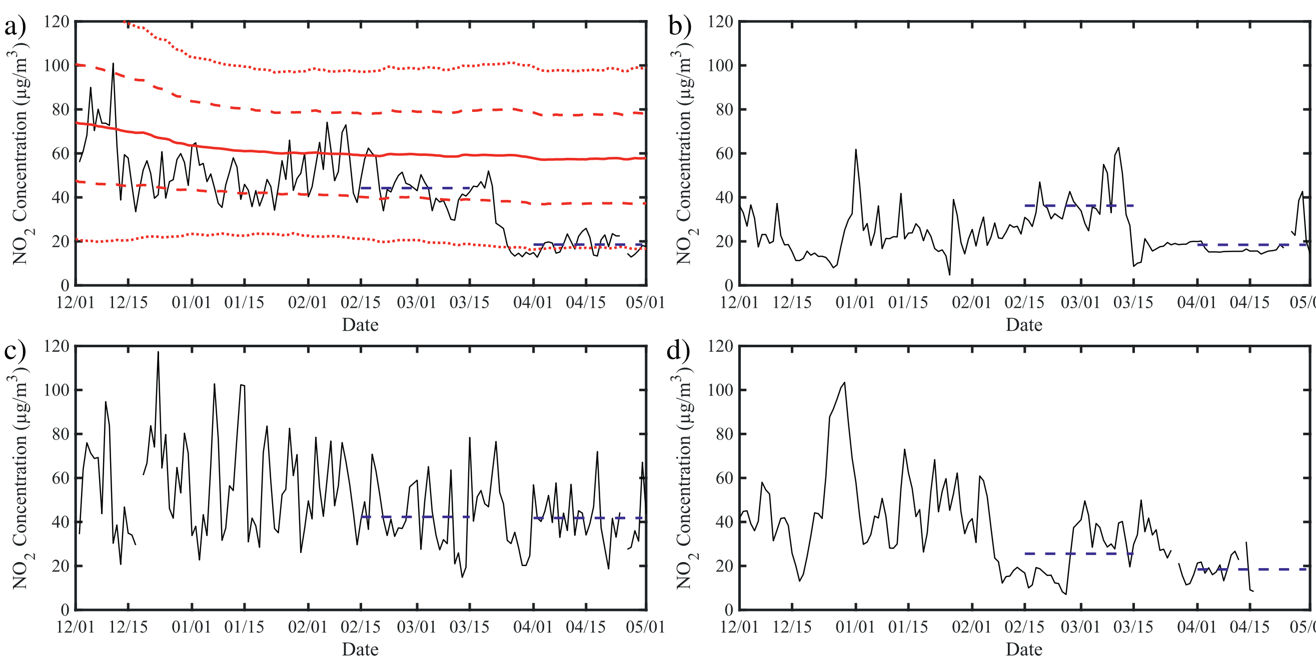

Figure 3. Time series of surface NO_2 concentration (μg/m^3) across the region of interest for the period December 1, 2019–May 1, 2020. Results are shown for: (a) Delhi; (b) Ludhiana; (c) Singrauli and (d) Asansol. The blue dashed lines represent the means over February 15–March 15 and April 1–30. In (a) the red curve is the climatological daily mean concentration based on available data 2005–2019 with the red dashed/dotted curves representing one/two standard deviation above and below the climatological mean. A 31 days moving window smoother has been applied to the climatological data.

However, the marked reduction in surface NO_2 concentrations observed in Delhi and Ludhiana were not uniform across the IGP. Singrauli, a city with a number of large coal-fired power plants in its vicinity (Singh et al., 2018), recorded no significant reduction in surface NO_2 concentrations, i.e., the means over the period February 15–March 15, 2020 and April 1–30, 3030 were both 42 μg/m^3, suggesting that the emissions from these plants were not reduced during the lockdown (Figure 3c). Asansol, a major industrial city with significant coal mining and steel production activities (Reddy & Ruj, 2003), in West Bengal showed a reduction in surface NO_2 values, from 25 μg/m^3 over the period February 15–March 15, 2020 to 18 μg/m^3 over the period April 1–30, suggesting a more modest lockdown than what occurred in Delhi and Ludhiana (Figure 3d).

Time series of pm2.5 concentrations from U.S. embassies and consulates throughout the IGP (Figure 4) indicates the presence of step function reductions in both Delhi as well as Lahore Pakistan, confirming that a lockdown also occurred in the Pakistani region of the IGP. Dhaka also showed a reduction however no indication of a step function change. This is most likely a reflection of the strong seasonality in air quality in the region with a winter peak associated with kiln production (Begum et al., 2011). There was also evidence of a step function response in Kathmandu although there was significant variability throughout April indicating either an incomplete shutdown of industrial activity or the long-range transport of pollution into the area (Bonasoni et al., 2012).

The climatological distribution of monthly mean tropospheric NO_2 column densities from OMI during April (Figure 5a) shows elevated levels across the IGP with lower levels over eastern India, southwestern India and Tibet. There is a gradient in density across the Himalaya that approximately follows the 3000 m height contour suggesting that topography plays a role in the distribution of air pollution across the region. A number of localized maxima associated with urban centers, like Delhi, Lahore, and Dhaka, or regions of industrial activity, such as Singrauli and Asansol are evident. The distribution during April 2020 (Figure 5b) shows generally lower values across much of the IGP with a marked absence of local maxima in the vicinity of Delhi and Lahore.

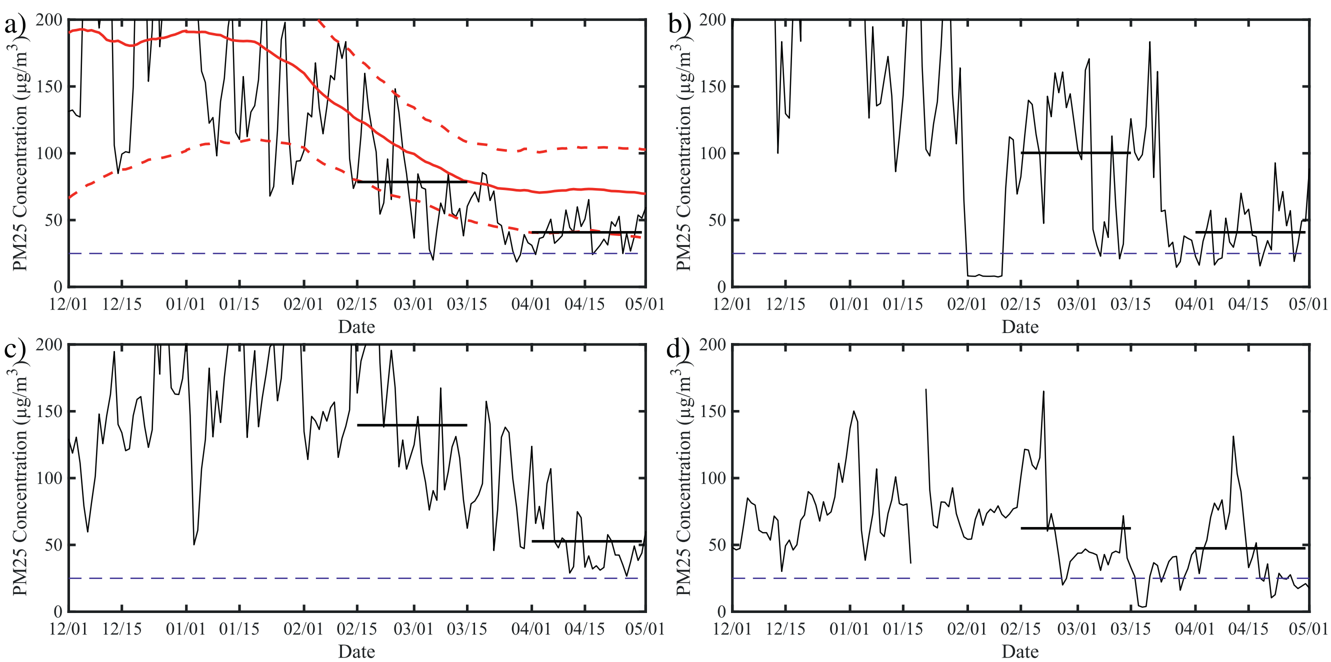

Figure 4. Time series of surface pm2.5 (μg/m^3) at selected sites in the region of interest for the period December 1, 2019–April 24, 2020. Results are shown for: (a) Delhi; (b) Lahore; (c) Dhaka and (d) Kathmandu. The blue dashed lines represent the mean over February 15–March 15 and April 1–30. In (a) the red curve is the climatological daily mean concentration based on available data 2016–2019 with the red dashed curves representing one standard deviation above and below the climatological mean. A 31 days moving window smoother has been applied to the climatological data. Also shown with the dashed blue line is the WHO standard for acceptable daily mean concentration (25 mg/m^3). WHO, World Health Organization.

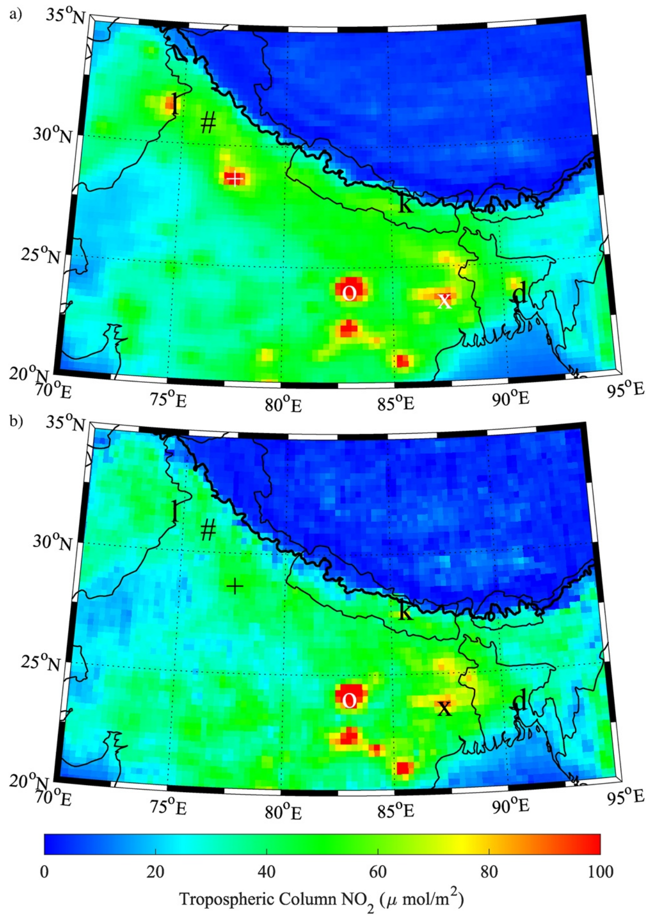

Figure 5. Column tropospheric NO_2 density from the OMI (m mol/m2) across the region of interest. Results are shown for: (a) April 1–30 climatology over 2005–2020 and (b) April 1–30, 2020. The locations of New Delhi ("+"), Ludhiana ("#"), Singrauli ("o"), Asansol ("x"), Lahore ('l), Kathmandu ("k") and Dhaka ("d") are indicated. Political boundaries are shown by the thin black curves with the 3000 m topographic height shown by the thick black curve. OMI, ozone monitoring instrument.

More information on the spatial variability on tropospheric NO_2 column densities associated with the lockdown is provided by the monthly mean anomaly during April 2020 (Figure 6a), i.e., the difference between the monthly mean during April 2020 and the April climatological monthly mean for the period 2005–2020. The widespread reduction across the northwestern IGP as well as adjoining foothills of the western Himalaya, i.e., to the west of Kathmandu, is evident. The region around Singrauli stands out as one in which there was a marked increase in column density during April 2020. Throughout much of the eastern IGP, including much of Bangladesh, eastern India, eastern Nepal and Bhutan, there was an increase in column density with the exception of region around Dhaka.

There is of course variability from year to year in air quality that is a function of variability in sources as well as meteorological conditions (Fishman et al., 2005; Pawar et al., 2017). One way to assess the magnitude of the anomalous tropospheric NO_2 column densities during April 2020 is to compare it to the expected variability from year to year during April. This so-called normalized anomaly is constructed by dividing the April 2020 anomaly by the standard deviation of the tropospheric NO_2 column density during April and expressing it as a percentage (Figure 6b). Normalized anomaly values on the order of $\pm$200% indicate that such an anomaly has a magnitude of 2 standard deviations and should, assuming normally distributed data, occur approximately 2%–3% of the time. Across much of the western IGP, including Delhi, Ludihana, and Lahore, as well as the western Himalaya, the normalized anomaly was on the order of 200% confirming the extreme reduction in air pollution in this region, a result in agreement with the surface observations of

10.1029/2020GH000351

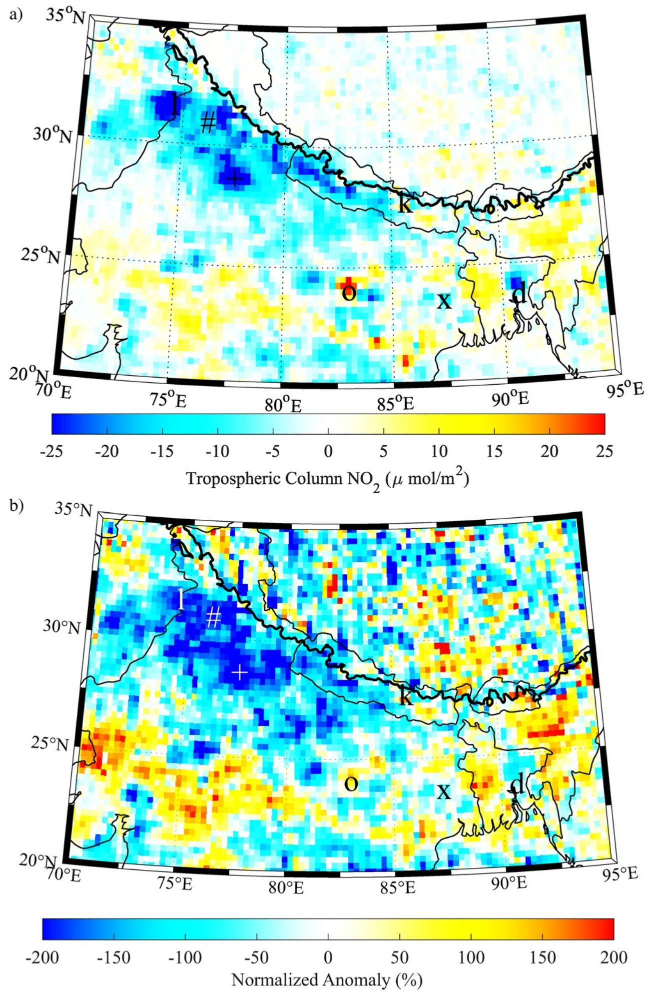

Figure 6. Anomalous column tropospheric NO_2 density from the OMI across the region of interest during April 2020. Results are shown for the: (a) anomaly (μ mol/m^2) (b) the normalized anomaly (%). The locations of New Delhi ("+"), Ludhiana ("#"), Singrauli ("o"), Asansol ("x"), Lahore ('l), Kathmandu ("k") and Dhaka ("d") are indicated. Political boundaries are shown by the thin black curves with the 3000 m topographic height shown by the thick black curve.

surface NO_2 concentration (Figure 3) and surface pm2.5 (Figure 4) across the western IGP. In contrast, the normalized anomaly across much of the eastern IGP and the eastern Himalaya was positive with values between 100% and 200% indicating that air pollution values in this region were anomalously high, although with significance levels lower than that in the west of the region of interest. This result is also in agreement with regional surface NO_2 concentrations during the lockdown (Figure 3) that show lower concentrations in Delhi and Ludhiana as well as higher concentrations in Singrauli and Asansol. We will refer to this feature, reduction in air pollution in the western IGP and Himalaya and an increase in the corresponding eastern regions, as an air pollution dipole anomaly.

Figure 5 and 6 indicate that there is evidence of spatial gradients in tropospheric NO_2 column densities along the Himalaya that may be under resolved by the OMI instrument. A comparison between TROPOMI monthly means for April 2019 and 2020 (Figure 7a and 7b) show clear evidence of a reduction in tropospheric NO_2 column densities across much of the IGP, including in the vicinity of Delhi, Lahore, Asansol, and Dhaka, as well as pronounced spatial gradients along the Himalaya. The difference between the two Aprils (Figure 7c) highlights the aforementioned dipolar nature of the changes that occurred with reductions across much of the western IGP and the western Himalaya and increases in the eastern areas of these regions.

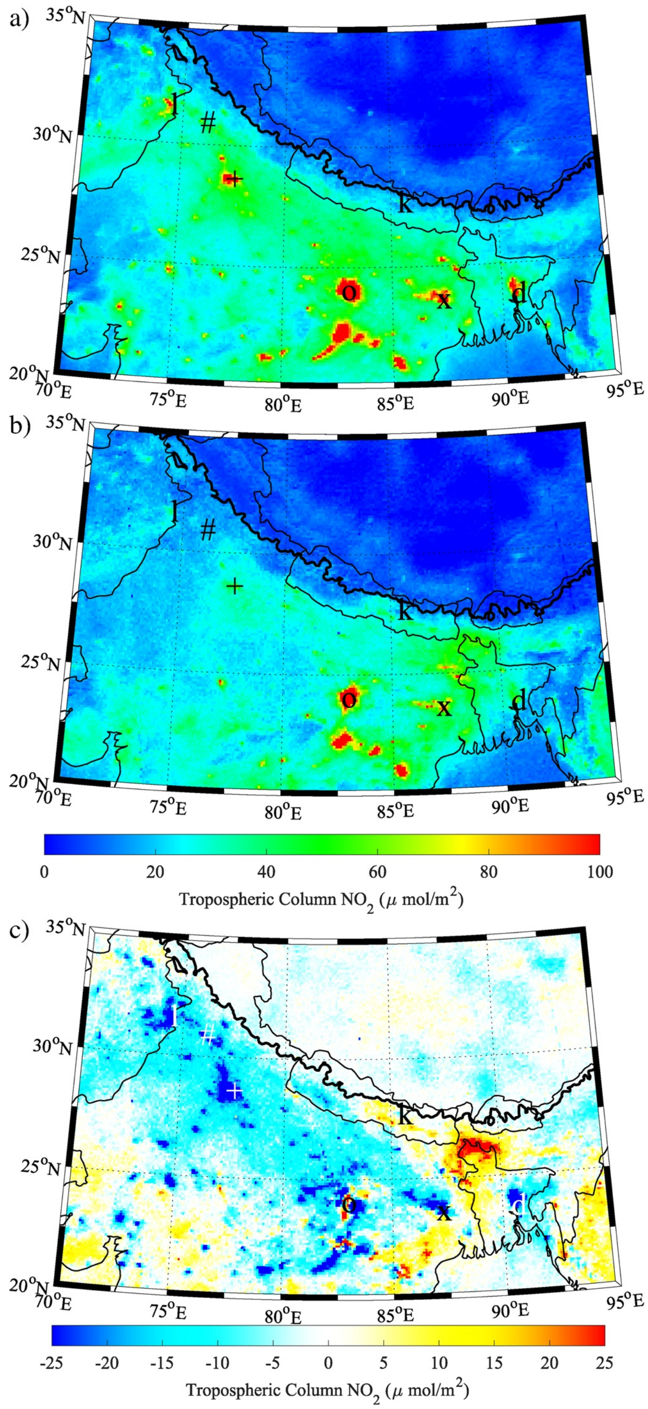

Figure 7. Column tropospheric NO2 density (μ mol/m^2) from the TROPOMI across the region of interest. Results are shown for: (a) April 1–30, 2019; (b) April 1–30, 2020 and (c) the difference between April 1–30, 2020 and 2019. The locations of New Delhi ("+"), Ludhiana ("#"), Singrauli ("o"), Asansol ("x"), Lahore ('l), Kathmandu ("k") and Dhaka ("d") are indicated. Political boundaries are shown by the thin black curves with the 3000 m topographic height shown by the thick black curve. TROPOMI, TROPOspheric Monitoring.

Observations of surface particulate matter (Figure 4) also indicated the presence of step function responses across the western IGP and Nepal that were associated with the lockdown. The climatological monthly mean AI for April (Figure 8a) indicates the presence of aerosols across the western IGP with lower values over Tibet. This pattern is the characteristic of so-called Atmospheric Brown Clouds, polluted tropospheric

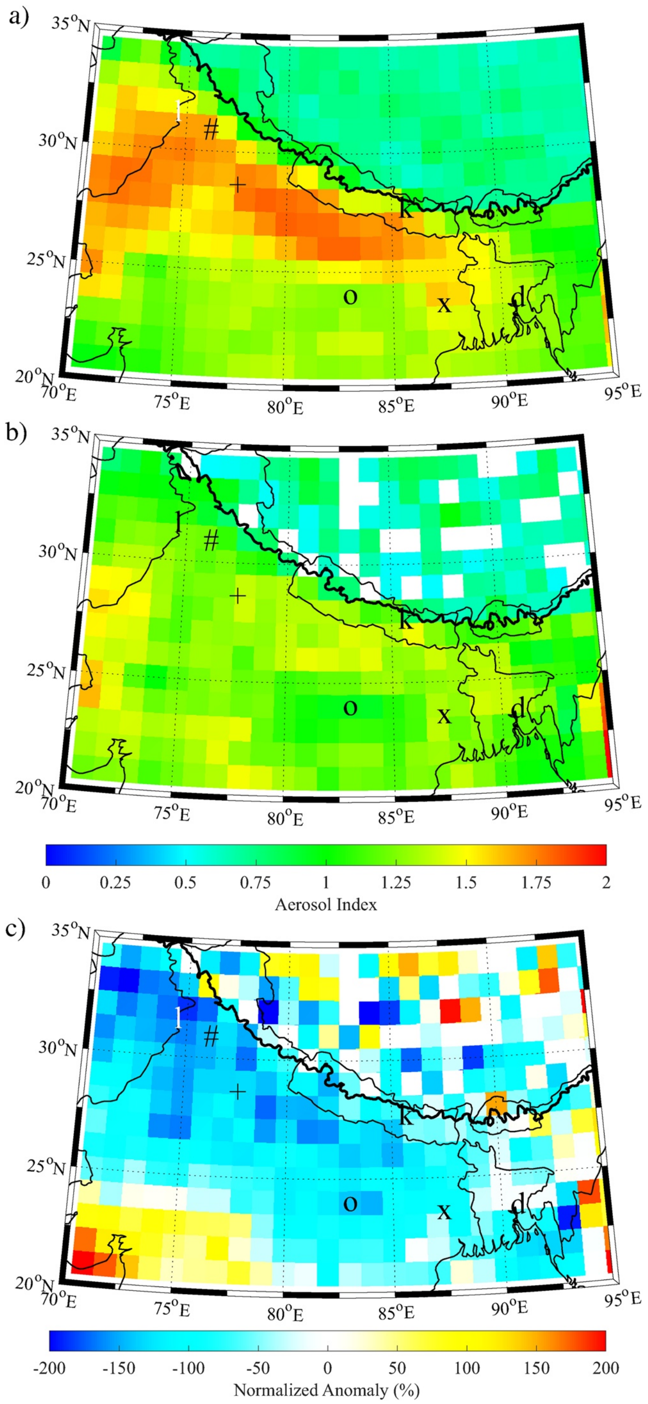

Figure 8. The Aerosol Index from OMI across the region of interest. Results are shown for: (a) April 1–30 climatology over 2005–2020; (b) April 1–30, 2020 and (c) the normalized anomaly (%) for April 1–30, 2020. The locations of New Delhi ("+"), Ludhiana ("#"), Singrauli ("o"), Asansol ("x"), Lahore ('l), Kathmandu ("k") and Dhaka ("d") are indicated. Political boundaries are shown by the thin black curves with the 3000 m topographic height shown by the thick black curve. OMI, ozone monitoring instrument.

layers characterized by high values of anthropogenic aerosols (Bonasoni et al., 2012; Ramanathan et al., 2007). The monthly mean AI for April 2020 (Figure 8b) shows reduced AI values across the IGP, consistent with the in situ observations of surface pm2.5 (Figure 3). The normalized anomaly for April 2020 (Figure 8c) indicates that the reduction in AI across the western IGP and the western Himalaya was between 1 and 1.5 standard deviations below the mean. Unlike the case for the tropospheric NO2 column density, these is no evidence of a coherent dipolar pattern with higher values of the AI in the eastern regions of the IGP and the Himalaya.

Atmospheric circulation patterns play a role in the long-range transport of pollutants into relatively pristine regions such as the Himalaya (Bonasoni et al., 2012). As such is it important to characterize the degree to which the atmospheric conditions contributed to the spatial distribution of the air pollution anomalies associated with the COVID-19 lockdown across the IGP. Figure 9 shows the April 2020 monthly mean anomaly in mass weighted velocity field, representative of circulation in the lower troposphere, over the region of interest as represented in the ERA5 reanalysis (Hersbach et al., 2020). It indicates the presence of a cyclonic (i.e., counter-clockwise) circulation anomaly over the region. A cyclonic circulation anomaly would have acted to mitigate the transport of pollutants from the IGP toward the western Himalaya and enhance this transport toward the eastern Himalaya. As such, it would have acted to support the existence of the dipolar pattern in the distribution of pollutants along the IGP and Himalaya during April 2020.

4. Conclusions

High mountainous regions of the world, traditionally, have been considered some of the most pristine environments and the least likely setting for hazards related to air pollution. However unique communities in high-altitude regions, such as those in the Himalaya, are unexpectedly exposed to pollution levels that are similar to, if not higher than, those reported in industrialized cities and other polluted environments (Saikawa et al., 2019). However little is known about the sources for this pollution and its pathways (Bonasoni et al., 2012). In addition, hypoxia and other unique characteristics of this high altitude ecosystem have compounding consequences for those who reside in and work in this region (Korrick et al., 1998; Pandey, 1984; Semple et al., 2016).

The COVID-19 lockdown within the heavily polluted IGP provides a unique opportunity to assess the impact of pollution from this region on the Himalaya. The lockdown produced a dipolar signature in pollution levels across the IGP with reductions in the west, that were two standard deviations below the climatological mean during April 2020 and a more modest increase in the east. This was most likely the result of differences in the local response to the lockdown with large cities such as Delhi and Lahore experiencing a reduction in activities such as transportation and construction that are sources of urban air pollution (Dhammapala, 2019; Mohan & Kandya, 2007); while industrial emitters such as those associated with steel production and power generation in the east continued (Reddy & Ruj, 2003; Singh et al., 2018). Changes in biomass burning during 2020 across the IGP may have also contributed to the signal (Gutti-

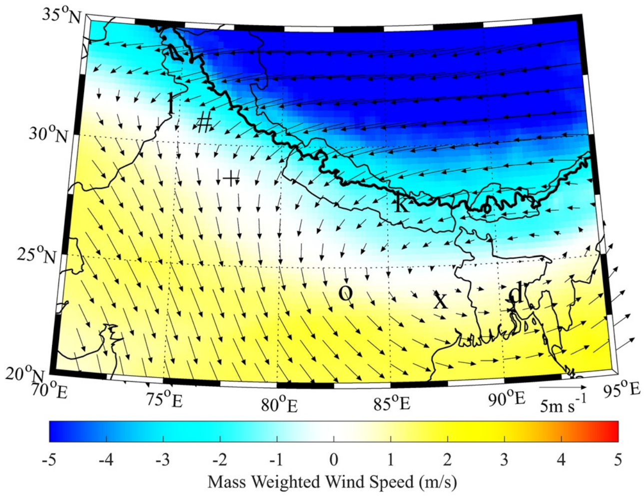

Figure 9. The tropospheric circulation across the region of interest during April 2020. The anomaly in the mass weighted wind (m/s) is shown. The locations of New Delhi ("+"), Ludhiana ("#"), Singrauli ("o"), Asansol ("x"), Lahore ('l), Kathmandu ("k") and Dhaka ("d") are indicated. Political boundaries are shown by the thin black curves with the 3000 m topographic height shown by the thick black curve.

kunda & Nishadh, 2020). A similar pattern was seen along the Himalaya with decreases in the west and increases in the east.

This pattern is also consistent with anecdotal observations indicating that, for the first time in recent history, the visibility of Himalayan peaks from India's National Capital region (Chamas, 2020; Ellis-Petersen et al., 2020). It is also consistent with other reports of the impact of the COVID-19 lockdown on regional air quality (Biswal et al., 2020; Kumar et al., 2020; Sharma et al., 2020).

A persistent atmospheric anomaly characterized by cyclonic (counter-clockwise) air flow throughout the lower troposphere during April 2020 contributed to the dipolar pattern seen in both the IGP and Himalaya. These results confirm the importance of characterizing the spatial distribution of emissions across the IGP as well as the background atmospheric circulation when assessing the impact of pollution on the Himalaya. They also provide an important test case that can be used to assess the ability of chemical transport models to capture regional patterns in air quality in the presence of large-scale changes in emissions (Moorthy et al., 2013; Sharma et al., 2017).

Conflict of Interest

The authors declare no conflicts of interest relevant to this study.

Data Availability Statement

All satellite data was accessed through the NASA Goddard Earth Sciences (GES) Data and Information Services Center (disc.gsfc.nasa.gov). Surface NO_2 data is available from the OpenAQ Platform (openaq.org) and the Indian Open Government Data Platform (data.in.gov). Data on pm2.5 concentrations is available through the U.S. Environmental Protection Agency (airnow.gov/international/us-embassies-and-consulates). ERA5 data is available through the Copernicus Climate Data Store (cds.climate.copernicus.eu).

Acknowledgments
G.W.K. Moore was supported by the Natural Sciences and Engineering Research Council of Canada.

References

Aplin, K. L., Scott, C. J., & Gray, S. L. (2016). Atmospheric changes from solar eclipses. *Philosophical Transactions of the Royal Society A: Mathematical, Physical and Engineering Sciences*, *374*(2077). 20150217. Retrieved from https://royalsocietypublishing.org/doi/abs/10.1098/rsta.2015.0217

Begum, B. A., Biswas, S. K., & Hopke, P. K. (2011). Key issues in controlling air pollutants in Dhaka, Bangladesh. *Atmospheric Environment*, *45*(40), 7705–7713. Retrieved from http://www.sciencedirect.com/science/article/pii/S1352231010008848

Biswal, A., Singh, V., Singh, S., Kesarkar, A. P., Ravindra, K., Sokhi, R. S., et al. (2020). COVID-19 lockdown induced changes in NO_2 levels across India observed by multi-satellite and surface observations. *Atmospheric Chemistry and Physics Discussions*, *2020*, 1–28. Retrieved from https://acp.copernicus.org/preprints/acp-2020-1023/

Boersma, K. F., Eskes, H. J., Dirksen, R. J., van der A, R. J., Veefkind, J. P., Stammes, P., et al. (2011). An improved tropospheric NO_2 column retrieval algorithm for the Ozone Monitoring Instrument. *Atmospheric Measurement Techniques*, *4*(9), 1905–1928. https://doi.org/10.5194/amt-4-1905-2011

Bonasoni, P., Cristofanelli, P., Marinoni, A., Vuillermoz, E., & Adhikary, B. (2012). Atmospheric pollution in the Hindu Kush-Himalaya Region. *Mountain Research and Development*, *32*(4), 468–479. https://doi.org/10.1659/mrd-journal-d-12-00066.1

Brasseur, G., & Granier, C. (1992). Mount Pinatubo aerosols, chlorofluorocarbons, and ozone depletion. *Science*, *257*(5074), 1239–1242. https://doi.org/10.1126/science.257.5074.1239

Chamas, Z. (2020). *Peaks of Himalayas visible from parts of India for first time in decades as pollution drops amid lockdown*. Australian Broadcasting Corporation. Retrieved from https://www.abc.net.au/news/2020-04-09/himalayas-visible-india-pollution/12136856

Dentener, F., Stevenson, D., Ellingsen, K., Van Noije, T., Schultz, M., Amann, M., et al. (2006). The global atmospheric environment for the next generation. *Environmental Science and Technology*, *40*(11), 3586–3594. https://doi.org/10.1021/es0523845

Dhammapala, R. (2019). Analysis of fine particle pollution data measured at 29 US diplomatic posts worldwide. *Atmospheric Environment*, *213*, 367–376. https://doi.org/10.1016/j.atmosenv.2019.05.070

Ellis-Petersen, H., Ratcliffe, R., Cowie, W., Daniels, J. P., & Kuo, L. (2020). *It's positively alpine!': Disbelief in big cities as air pollution falls*. The Guardian.

Fishman, J., Creilson, J. K., Wozniak, A. E., & Crutzen, P. J. (2005). Interannual variability of stratospheric and tropospheric ozone determined from satellite measurements. *Journal of Geophysical Research: Atmosphere*, *110*(D20). Retrieved from https://agupubs.onlinelibrary.wiley.com/doi/abs/10.1029/2005JD005868

Ghude, S. D., Kulkarni, P. S., Kulkarni, S. H., Fadnavis, S., & Van Der A, R. J. (2011). Temporal variation of urban NOx concentration in India during the past decade as observed from space. *International Journal of Remote Sensing*, *32*(3), 849–861. https://doi.org/10.1080/01431161.2010.517797

Guttikunda, S. K., & Nishadh, K. A. (2020). *Air quality trends and lessons learned in India during the COVID lockdowns*. Delhi, India: Collaborative Clean Air Policy Centre. Retrieved from https://ccapc.org.in/policy-briefs/2020/aq-changes-lockdown

Hersbach, H., Bell, B., Berrisford, P., Hirahara, S., Horányi, A., Muñoz-Sabater, J., et al. (2020). The ERA5 global reanalysis. *Quarterly Journal of the Royal Meteorological Society*, *146*(730), 1999–2049. Retrieved from https://rmets.onlinelibrary.wiley.com/doi/abs/10.1002/qj.3803

Hong, G., Yang, P., Minnis, P., Hu, Y. X., & North, G. (2008). Do contrails significantly reduce daily temperature range? *Geophysical Research Letters*, *35*(23). https://doi.org/10.1029/2008gl036108

Korrick, S. A., Neas, L. M., Dockery, D. W., Gold, D. R., Allen, G. A., Hill, L. B., et al. (1998). Effects of ozone and other pollutants on the pulmonary function of adult hikers. *Environmental Health Perspectives*, *106*(2), 93–99. https://doi.org/10.1289/ehp.9810693

Kumar, P., Hama, S., Omidvarborna, H., Sharma, A., Sahani, J., Abhijith, K. V., et al. (2020). Temporary reduction in fine particulate matter due to 'anthropogenic emissions switch-off' during COVID-19 lockdown in Indian cities. *Sustainable Cities and Society*, *62*, 102382. Retrieved from https://www.sciencedirect.com/science/article/pii/S221067072030603X

Lau, W. K., & Kim, K. M. (2010). Fingerprinting the impacts of aerosols on long-term trends of the Indian summer monsoon regional rainfall. *Geophysical Research Letters*, *37*(16). https://doi.org/10.1029/2010gl043255

Lippmann, M. (1989). Health effects of ozone: A critical review. *JAPCA*, *39*(5), 672–695. https://doi.org/10.1080/08940630.1989.10466554

Mohan, M., & Kandya, A. (2007). An analysis of the annual and seasonal trends of air quality index of Delhi. *Environmental Monitoring and Assessment*, *131*(1-3), 267–277. https://doi.org/10.1007/s10661-006-9474-4

Moore, G., & Semple, J. (2009). High concentration of surface ozone observed along the Khumbu Valley Nepal April 2007. *Geophysical Research Letters*, *36*(14). https://doi.org/10.1029/2009gl038158

Moorthy, K. K., Beegum, S. N., Srivastava, N., Satheesh, S. K., Chin, M., Blond, N., et al. (2013). Performance evaluation of chemistry transport models over India. *Atmospheric Environment*, *71*, 210–225. Retrieved from http://www.sciencedirect.com/science/article/pii/S1352231013000812

Pandey, M. R. (1984). Prevalence of chronic bronchitis in a rural community of the Hill Region of Nepal. *Thorax*, *39*(5), 331–336. https://doi.org/10.1136/thx.39.5.331

Pawar, V. S., Domkawale, M. A., Pawar, S. D., Salvekar, P. S., & Pradeep Kumar, P. (2017). Inter annual variability of tropospheric NO2 and tropospheric ozone over Maharashtra (India): The role of lightning. *Remote Sensing Letters*, *8*(11), 1015–1024. https://doi.org/10.1080/2150704x.2017.1346398

Ramanathan, V., Ramana, M. V., Roberts, G., Kim, D., Corrigan, C., Chung, C., & Winker, D. (2007). Warming trends in Asia amplified by brown cloud solar absorption. *Nature*, *448*(7153), 575–578. https://doi.org/10.1038/nature06019

Reddy, G. S., & Ruj, B. (2003). Ambient air quality status in Raniganj-Asansol area, India. *Environmental Monitoring and Assessment*, *89*(2), 153–163. https://doi.org/10.1023/a:1026070506481

Saikawa, E., Panday, A., Kang, S., Gautam, R., Zusman, E., Cong, Z., et al. (2019). Air Pollution in the Hindu Kush Himalaya. In P. Wester, A. Mishra, A. Mukherji, & A. B. Shrestha, (Eds.), *The Hindu Kush Himalaya assessment: Mountains, climate change, sustainability and people* (pp. 339–387). Cham: Springer International Publishing.

Semple, J. L., Moore, G. W. K., Koutrakis, P., Wolfson, J. M., Cristofanelli, P., & Bonasoni, P. (2016). High concentrations of ozone air pollution on Mount Everest: Health implications for Sherpa communities and mountaineers. *High Altitude Medicine & Biology*, *17*(4), 365–369. https://doi.org/10.1089/ham.2016.0042

Sharma, S., Sharma, P., & Khare, M. (2017). Photo-chemical transport modeling of tropospheric ozone: A review. *Atmospheric Environment*, *159*, 34–54. Retrieved from http://www.sciencedirect.com/science/article/pii/S1352231017302170

Sharma, S., Zhang, M., Anshika, J., Gao, J., Zhang, H., & Kota, S. H. (2020). Effect of restricted emissions during COVID-19 on air quality in India. *The Science of the Total Environment*, *728*, 138878. Retrieved from https://www.sciencedirect.com/science/article/pii/S0048969720323950

Singh, R., Kumar, S., & Singh, A. (2018). Elevated black carbon concentrations and atmospheric pollution around Singrauli coal-fired thermal power plants (India) using ground and satellite data. *International Journal of Environmental Research and Public Health*, *15*(11), 2472. https://doi.org/10.3390/ijerph15112472

Torres, O., Tanskanen, A., Veihelmann, B., Ahn, C., Braak, R., Bhartia, P. K., et al. (2007). Aerosols and surface UV products from Ozone Monitoring Instrument observations: An overview. *Journal of Geophysical Research: Atmosphere*, *112*(D24). Retrieved from https://agupubs.onlinelibrary.wiley.com/doi/abs/10.1029/2007JD008809

Travis, D. J., Carleton, A. M., & Lauritsen, R. G. (2004). Regional variations in U.S. diurnal temperature range for the 11-14 September 2001 aircraft groundings: Evidence of Jet Contrail Influence on Climate. *Journal of Climate*, *17*(5), 1123–1134. https://doi.org/10.1175/1520-0442(2004)017<1123:rviudt>2.0.co;2

Veefkind, J. P., Aben, I., McMullan, K., Förster, H., De Vries, J., Otter, G., et al. (2012). TROPOMI on the ESA Sentinel-5 Precursor: A GMES mission for global observations of the atmospheric composition for climate, air quality and ozone layer applications. *Remote Sensing of Environment*, *120*, 70–83. https://doi.org/10.1016/j.rse.2011.09.027

WHO (2006). *Air quality guidelines for particulate matter, ozone, nitrogen dioxide and sulfur dioxide: Global update 2005: Summary of risk assessment*. World Health Organization. Retrieved from https://apps.who.int/iris/handle/10665/69477